Revista Eletrônica Paulista de Matemática

ISSN 2316-9664
Volume 10, dez. 2017
Edição Ermac

Automatic construction of 3D models of arterial tree incorporating the Fåhraeus-Lindqvist effect

Patricia Fonseca de Brito
Graduate Program in Computational Modelling, Federal University of Juiz de Fora (UFJF)
patriciafonseca@ice.ufjf.br

Lucas Diego Mota Meneses
Graduate Program in Computational Modelling, Federal University of Juiz de Fora (UFJF)
lucasmeneses@ice.ufjf.br

Rodrigo Weber dos Santos
Graduate Program in Computational Modelling, Federal University of Juiz de Fora (UFJF)
rodrigo.weber@ufjf.edu.br

Rafael Alves Bonfim de Queiroz
Graduate Program in Computational Modelling, Federal University of Juiz de Fora (UFJF)
rafael.bonfim@ice.ufjf.br

Abstract

Arterial tree models have been successfully used to obtain a better understanding of all aspects hemodynamics of clinically relevant regions of the human body in order to diagnosis and applications in surgical planning. Basically, the models can be classified into: anatomical, lumped parameter, fractal and optimized. This work focuses on the generation of 3D optimized models based on Constructive Constrained Optimization (CCO) method equipped with a model to account for the Fåhraeus-Lindqvist effect, which indicates that the blood viscosity depends on the diameter of the vessel and discharge hematocrit through a nonlinear function. In this work, data morphometrics from models are compared with those of real coronary trees and the effective admittance of the models is investigated.
Keywords: Coronary arterial tree. Fåhraeus-Lindqvist effect. Computational modeling. Effective admittance.

Resumo

Modelos de árvores arteriais têm sido utilizados com sucesso para obter uma melhor compreensão de todos os aspectos relacionados à hemodinâmica de regiões do corpo humano, passando pelo diagnóstico e com aplicações no planejamento cirúrgico. Basicamente, os modelos podem ser classificados em: anatômico, parâmetro condensado, fractal e otimizado. Neste trabalho, foca-se na geração de modelos otimizados 3D baseados no método CCO (Constructive Constrained Optimization) equipado com o efeito Fåhraeus-Lindqvist, o qual indica que a viscosidade sanguínea depende do diâmetro do vaso e da descarga de hematócrito através de uma função não linear. Neste trabalho, dados morfométricos dos modelos são comparados com aqueles de árvores coronarianas reais e a admitância efetiva dos modelos é investigada.
Palavras-chave: Árvore arterial coronariana. Efeito Fåhraeus-Lindqvist. Modelo computacional. Admitância efetiva.

1 Introduction

Arterial trees serve to the purpose of conveying blood to all sites of a tissue. Hemodynamic simulation studies use computational models of arterial trees as their geometrical substrate. These studies have been used to gain a better understanding of all aspects related to blood flow, from wave propagation and analysis of pressure pulse can be used for diagnosis and surgical planning applications. To date these simulations can employ one of following class of arterial tree models: lumped parameter models (MATES; KLOCKE; CANTY JR, 1988), anatomical models (WATANABE; BLANCO; FEIJÓO, 2013), fractal models (VAN BEEK; ROGER; BASSINGTHWAIGHTE, 1989; YANG; WANG, 2013) and optimized (SCHREINER; BUXBAUM, 1993; KARCH et al., 1999; SCHWEN et al., 2015; BRITO, 2016).

In particular, this work is interested in optimized models generated by method of Constrained Constructive Optimization (CCO) (SCHREINER; BUXBAUM, 1993; KARCH et al., 1999; QUEIROZ, 2013; BRITO, 2016). Arterial tree models generated by CCO are able to mimic important properties of real arterial trees, such as segment radii, branching angle statistics and pressure profiles. However, the CCO method is not able to take into account the Fåhraeus-Lindqvist effect during the generation of the models, which is an effect where the viscosity of the blood changes with the diameter of the vessel and discharge hematocrit it travels through (FÅHRAEUS; LINDQVIST, 1931). For example, there is a decrease of viscosity as the vessel's diameter decreases when the vessel diameter is between 10 and 300 micrometers.

In this context, the purpose of this work is to provide an algorithm based on CCO method that generates arterial tree models considering the Fåhraeus-Lindqvist effect. The models obtained by the algorithm are compared with morphometric data of real coronary arterial trees. Detailed investigation of the algorithm can be seen in (BRITO, 2016). Furthermore, the root effective admittance of models was calculated in order to investigate the impact of the number of terminal segments of models in this dynamic property. It is obtained using an iterative formula based on theoretical result of Duan and Zamir (DUAN; ZAMIR, 1995).

It is important inform that preliminary results were presented recently at ERMAC 2017 (BRITO et al., 2017). In this actual work are described: (i) an algorithm that describes an iterative process to calculate the blood viscosity through a nonlinear function, (ii) it provides results of models generated considering linear and nonlinear blood viscosities, and (iii) it depicts the root effective admittance of arterial trees models.

The remainder of this paper is organized as follows. In Section 2, the algorithm proposed based on CCO method is described. In Section 3, it is presented the procedure to determine the root effective admittance. In Section 4, results obtained using the algorithm developed are presented. Section 5 contains our conclusion and discusses the future direction of this work.

2 The algorithm based on CCO

The algorithm here proposed is based on the assumptions and constraints listed below (SCHREINER; BUXBAUM, 1993; KARCH et al., 1999; QUEIROZ, 2013):

- The concept associated with the construction is to minimize the total intravascular volume

$$V = \pi \sum_{i=1}^{K_{tot}} l_i r_i^2, \tag{1}$$

where l_i and r_i are the length and radius of the segment i, K_{tot} is the number of segments of the tree in growth stage;

- the tree model is generated on a fixed 3D domain non necessarily convex Ω_{perf} that represents an organ;
- the proximal localization $\mathbf{x}_{prox}$ of the root segment (feeding artery) is known and fixed in the boundary of the domain at the beginning of the simulation;
- the arterial tree is modeled as a dichotomously branching (binary) system of straight cylindrical tubes (vessel segments);
- the model tree starts at the root segment (main feeding artery) and it is truncated in the form of terminal segments on prearteriolar level;
- the model tree should take up the space of the perfusion domain as homogeneously as possible without intersection of segments;
- the blood is modeled as an incompressible, homogeneous Newtonian fluid at steady state and laminar flow conditions (BATCHELOR, 2000);
- at bifurcations the radii of parent (r_p) and daughter segments (r_{dl}, r_{dr}) are forced to exactly fulfill a bifurcation law derived from real coronary trees (ZAMIR, 1988):

$$r_p^{\gamma} = r_{dl}^{\gamma} + r_{dr}^{\gamma}, \tag{2}$$

where γ is a constant exponent with ranging between 2.55 and 3, governing the shrinkeage of radii across bifurcations;

- hydrodynamic resistance R of each segment of the tree is assumed to follow Poiseuille's law

$$R = \left(\frac{8\eta_i}{\pi}\right)\frac{l_i}{r_i^4}, \tag{3}$$

where η_i is the blood viscosity. The CCO method adopts $\eta_i = 3.6$ cP (constant). In this work the blood viscosity η_i is described as a non-linear function given by (PRIES et al., 1990):

$$\eta_i = \eta_p\left[1+(\eta_{0.45}-1)\left(\frac{d_i}{d_i-1.1}\right)^2\right]\left(\frac{d_i}{d_i-1.1}\right)^2, \tag{4}$$

where d_i is the diameter of the segment i, $\eta_p = 1.1245$ cP is the plasma viscosity, and $\eta_{0.45}$ is the apparent viscosity of the plasma for a discharge hematocrit of 0.45 given by

$$\eta_{0.45} = 6\exp(-0.085d_i) + 3.2 - 2.44\exp(-0.06d_i^{0.645}); \tag{5}$$

- the pressure drop Δp_s along each segment is given by

$$\Delta p_s = RQ, \tag{6}$$

where Q is the flow through segment;

- each terminal segment supplies an identical and equal amount of blood flow Q_{term} into the microcirculatory network, which is not modeled in detail;
- the overall pressure drop of the model is given by

$$\Delta p = p_{perf} - p_{term}, \tag{7}$$

where p_{perf} is the perfusion pressure at the inlet of the root segment, p_{term} is the pressure at the outlet of all the terminal segments;

- the radius of the root segment r_{iroot} is scaled during the growth of the tree model by CCO method as follows:

$$r_{iroot} = \left[R^*_{sub,iroot} \frac{Q_{perf}}{\Delta p} \right], \tag{8}$$

where $R^*_{sub,iroot}$ denotes the reduced hydrodynamic resistance of the whole tree (see details in (KARCH et al., 1999)) and $Q_{perf} = k_{term} Q_{term}$ which k_{term} denotes the number of terminal segments to be supplied.

The algorithm of tree generation based on CCO method has previously been described in detail by BRITO (2016). The generation of the model starts by planting the root segment (*iroot*) with its proximal end $\mathbf{x}_{prox}$ fixed at the perfusion domain Ω_{perf} and the distal $\mathbf{x}_{inew}$ selected randomly within this domain. If this position is not too close to $\mathbf{x}_{prox}$, $\mathbf{x}_{inew}$ is connected to $\mathbf{x}_{prox}$, resulting in a root segment length (l_{iroot}). The radius r_{iroot} of the root segment is such that the hydrodynamic resistance $R^*_{sub,iroot}$ yields the flow $Q_{perf} = Q_{term}$ through one terminal segment, i.e., $k_{term} = 1$. At this moment, $R^*_{sub,iroot} = \frac{8\eta_i}{\pi} l_{iroot}$ and η_i assumes 3.6 cP to calculate radius r_{iroot}. In following, η_i is updated using Eq. (4) with $d_i = 2r_{iroot}$ and again the radius r_{iroot} is computed. The iterative procedure explained above is repeated until convergence is achieved with precision $\varepsilon = |r^{n+1}_{iroot} - r^n_{iroot}| < 10^{-5}$ for example, where n denotates iterations. The convergence denotes that the radius of the root segment does not change significantly between two iterations, consequently the blood viscosity was adequately updated in each segment. Related to the stopping criterion based on the number of iterations, the algorithm is terminated when the number of iterations reaches the maximum number of iterations, which have the value 10 in this work.

Given a tree with k_{term} terminal segments, the stepwise growing of the tree is as follows. First, the location $\mathbf{x}_{inew}$ for a new terminal is selected from a pseudorandom number sequence, uniformly distributed inside the perfusion domain. The prospective location $\mathbf{x}_{inew}$ is accepted as a candidate for a new terminal site only if $\mathbf{x}_{inew}$ satisfies a distance criterion (SCHREINER; BUXBAUM, 1993).

Since $\mathbf{x}_{inew}$ has been accepted as a distal end of a new terminal segment, it is temporarily connected to each of the neighboring segments, one after the other. Connecting the new terminal segment to a preexisting segment, consequently cause violation in the boundary condition regarding the terminal flows. In order to return the proper terminal flows, the flow resistance of the tree must be adjusted for each temporary connection. This can only be performed by rescaling of the segments' radii (KARCH et al., 1999) equipped with an iterative procedure that estimates and corrects the nonlinear viscosity in each segment of the tree. This iterative procedure is described in the Algorithm 2.

The bifurcation site resulting in each temporary connection is optimized in order to minimize the Eq. (1), as explained in Section 2.1, and dissolved again. After assessing all possible connections in the neighborhood of $\mathbf{x}_{inew}$, the connection that provided the lowest optimization target is

adopted as permanent for the new terminal site $\mathbf{x}_{inew}$. Thus, the tree is grown to $k_{term}+1$ terminal segments. The process of growing the tree summarized above is repeated until $k_{term} = N_{term}$, i.e., the preset number of terminals N_{term} is achieved. The steps described previously are systematized in the Algorithm 1.

2.1 Optimization of the bifurcation position

This stage of the algorithm determines a position for new bifurcation in order to minimize the Eq. (1). Firstly, the distal position of a new terminal segment $\mathbf{x}_{inew}$ is connected in the midpoint of a existent segment of the tree resulting in a new bifurcation. This bifurcation position should be modified in order to minimize the total intravascular volume. The method adopted here was developed by (QUEIROZ, 2013).

Suppose the distal position of a new terminal segment $\mathbf{x}_{inew} = (x_3, y_3, z_3)$ is connected in the midpoint of segment *icon* with distal position $\mathbf{x}_D = (x_2, y_2, z_2)$ and proximal position $\mathbf{x}_P = (x_1, y_1, z_1)$ (see Fig. 1). These points form the bifurcation plane containing optimum bifurcation (KARCH et al., 1999). To find this optimum position $\mathbf{x}_{ibif}$ in triangle Δ_1 was utilized isoparametric mapping. A point $G = (\varepsilon, \kappa)$ in triangle Δ_2 can be represented as a point $\mathbf{x}_{ibif} = (x, y, z)$ in triangle Δ_1 by equations:

$$x = \sum_{i=1}^{3} \phi_i(\varepsilon, \kappa) x_i, \quad y = \sum_{i=1}^{3} \phi_i(\varepsilon, \kappa) y_i, \quad z = \sum_{i=1}^{3} \phi_i(\varepsilon, \kappa) z_i, \tag{9}$$

where

$$\phi_1(\varepsilon, \kappa) = 1 - \varepsilon - \kappa, \quad \phi_2(\varepsilon, \kappa) = \varepsilon, \quad \text{and} \quad \phi_3(\varepsilon, \kappa) = \kappa. \tag{10}$$

Note that the vertices $\mathbf{x}_P$, $\mathbf{x}_D$ and $\mathbf{x}_{inew}$ of Δ_1 correspond the vertices G_1, G_2, G_3 of triangle Δ_2, respectively.

The triangle Δ_2 is partitioned by a regular mesh with spacing $\delta = \frac{1}{N_e}$ in directions κ and ε, where N_e is the previously selected parameter. In Figure 1, $N_e = 6$. The nodes of mesh are represented in triangle Δ_1 as $\mathbf{x}_{ibif}$ using Eq. (9) which are candidates for optimum bifurcation.

Given N_{pts} positions $\mathbf{x}_{ibif} = (x, y, z)$ in triangle Δ_1, each of them is used to create a temporary bifurcation. With each new bifurcation, the cost function (1) is computed. Finally, the position $\mathbf{x}_{ibif}$ that resulted in the lowest value of the cost function is considered optimal for connecting $\mathbf{x}_{inew}$ to the segment *icon*.

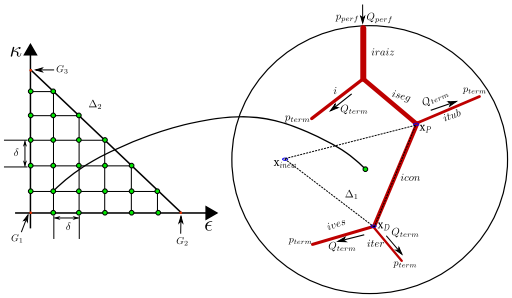

Figure 1: Example of determination the site bifurcation when adding a terminal segment.

Algorithm 1: Automatic generation of arterial tree models inspired in the CCO method.

Data: Ω_{perf}, $\mathbf{x}_{prox}$, Q_{perf}, N_{term}, γ.

Fix the proximal position $\mathbf{x}_{prox}$ of the root segment into domain Ω_{perf};
repeat
    Generate the distal position $\mathbf{x}_{inew}$ for the root segment into domain Ω_{perf};
    Distance criterion: check if this position is not too close to $\mathbf{x}_{prox}$;
until *(distance criterion is met)*;
Connect $\mathbf{x}_{inew}$ to $\mathbf{x}_{prox}$ (*planting the root segment*);
Update the viscosity of root segment through iterative procedure (Algorithm 2);
$k_{term} \leftarrow 1$;
while $(k_{term} < N_{term})$ **do**
    repeat
        Generate the distal position $\mathbf{x}_{inew}$ for a new terminal segment;
        Distance criterion: check if this position is not too close to any of the existing segments;
    until *(distance criterion is met)*;
    Obtain the neighboring segments N_{con} of $\mathbf{x}_{inew}$ for temporary connection;
    for $j \leftarrow 1$ ***to*** N_{con} **do**
        Connect $\mathbf{x}_{inew}$ to the midpoint $\mathbf{x}_{ibif}$ of segment j;
        Update the viscosity of segment through iterative procedure (Algorithm 2);
        Optimize the bifurcation position $\mathbf{x}_{ibif}$ (see details in Section 2.1);
        Perform restriction checks (e.g. segment intersection, segments traversing forbidden domains);
        Save value of target function, position $\mathbf{x}_{ibif}$ and results of check in line j of the *Connection Evaluation Table* (*CET*);
        Remove the bifurcation created;
    Restrict *CET* to allowed connections: CET^{v};
    if $(CET^{v}$ *is not an empty set)* **then**
        Find optimal connection j_{opt} from CET^{v} (*structural optimization*);
        Make connection from $\mathbf{x}_{inew}$ to j_{opt} permanent;
        Update the viscosity of segment through iterative procedure;
        $k_{term} \leftarrow k_{term} + 1$;
    else
        Refuse the position $\mathbf{x}_{inew}$;
Return the quantities calculated (length, radius, resistance, pressure drop, blood flow);

Algorithm 2: Iterative procedure (non-linear viscosity)

Data: Arterial tree with K_{term} terminal segments.

$K_{tot} = 2K_{term} - 1$;
Obtain the set $T = \{T_1, T_2, \ldots, T_{K_{term}}\}$ whose elements are the terminal segments;
repeat
  for $j = 1$ ***to*** K_{term} **do**
    for $i = 1$ ***to*** K_{tot} **do**
      if *the segment i is same to segment iroot* **then**
        Calculate the radius of the segment *iroot* by Eq. (8);
        $d_{iroot} = 2r_{iroot}$;
        Update the viscosity $\eta_{iroot} = \eta(d_{iroot})$ using Eq. (4);
      else
        Calculate the radius of the segment i (see (KARCH et al., 1999));
        $d_i = 2r_i$;
        Update the viscosity $\eta_i = \eta(d_i)$ using Eq. (4);
    for $i = T_j$ ***to*** *iroot and for all segment in this path* **do**
      if *the segment i is same to segment iroot* **then**
        Calculate the radius of the segment *iroot* by Eq. (8);
      else
        Calculate the radius of the segment i (see (KARCH et al., 1999));
until *the convergence criterion is reached*;

3 Procedure to determine the root effective admittance

The effective admittance of an arterial tree model is measure of its dynamic performance. It represents the extent to which a pressure or flow wave entering the tree would be admitted (ZAMIR, 2000). In following, the procedure to determine the root effective admittance is described in tree steps (DUAN; ZAMIR, 1995):

- **Step 1**: the characteristic admittance Y_i of each segment i in the model is calculated from the following relation

$$Y_i = \frac{A_i}{\rho c_i}, \tag{11}$$

  where A_i is the cross-sectional area of the segment i, ρ is the density of the fluid, and c_i is the wave speed in the segment i given by

$$c_i = \sqrt{\frac{Eh_i}{\rho d_i}}, \tag{12}$$

  where E is the Young's modulus, d_i is a diameter of segment i and h_i is the wall thickness of the segment i.

- **Step 2**: it is considered that effective admittance $Y_e{}^{term}$ of each terminal segment $term$ is identical to their characteristic admittances Y_{term}.

- **Step 3**: the root effective admittance Y_e^{iroot} is obtained marching backward along the tree structure and determining the effective admittance of each segment i

$$Y_e{}^i = Y_i \left[\frac{Y_e{}^{dl} + Y_e{}^{dr} + jY_i \tan(\omega \frac{l_i}{c_i})}{Y_i + j(Y_e{}^{dl} + Y_e{}^{dr}) \tan(\omega \frac{l_i}{c_i})} \right], \tag{13}$$

where j is the imaginary unit, l_i is the length of segment i, $\omega = 2\pi f$ is the angular frequency, f is the frequency, and $Y_e{}^{dl}$ and $Y_e{}^{dr}$ are effective admittance of daugthers left (dl) and right (dr) of segment i, respectively.

In Eq. (13), one can see that the effective admittance depends on frequency. For this reason it is necessary to obtain values of effective admittance of an arterial tree model at different frequencies, to produce a so called frequency spectrum, which is a dynamic profile of the tree (ZAMIR, 2000).

4 Results

In this section results obtained with the Algorithms 1 and 2 are presented. These algorithms were implemented using the programming language ANSI C. The computer simulations were performed in a Dell laptop with processor Intel Core i5, memory 8 GB and hard drive 1 TB.

4.1 Comparison with real coronary arterial trees

For morphometric comparison with real coronary arterial trees, the Algorithm 1 was applied to generate arterial trees with 250 terminal segments (499 in total) in order to represent the tree of the left anterior descending (LAD) coronary artery.

The arterial tree models were generated under the following conditions (KARCH et al., 1999): perfusion pressure $p_{perf} = 100$ mmHg, terminal pressure $p_{term} = 72$ mmHg, total perfusion flow $Q_{perf} = 500$ mL/min, terminal flows $Q_{term} = 2$ mL/min, bifurcation exponent $\gamma = 3$, spherical volume Ω_{perf} = 100 cm^3 representing tissue to be perfused (LAD region). Two case studies were performed using different viscosities: linear $\eta = 3.6$ cP and nonlinear given by Eq. (4).

For each simulation, ten replicates of the tree with 250 terminal segments were generated with the same predefined parameters. Each tree was generated using a different sequence of pseudorandom numbers for casting the distal ends of its terminal segments.

Figure 2 shows an arterial tree models generated with viscosity given by Eq (4). Note that the segments with larger radius have blood viscosity (Eq. (4)) near to 3.6 cP.

Figure 3 displays the mean diameter and standard deviation of this mean diameter (SDM) of all vessel segments at a certain bifurcation level, defined as the number of proximal bifurcations of a segment. This figure also shows the mean length and standard deviation of this mean length (SDM). Diamonds and triangles denote measurements from corrosion casts of the coronary networks of two human hearts (ZAMIR; CHEE, 1987). One can see in Fig. 3 that the results produced by the models are consistent with the experimental data (ZAMIR; CHEE, 1987). It was observed that the choice of blood viscosity did not significantly affect the distribution of the diameters and lengths of the segments.

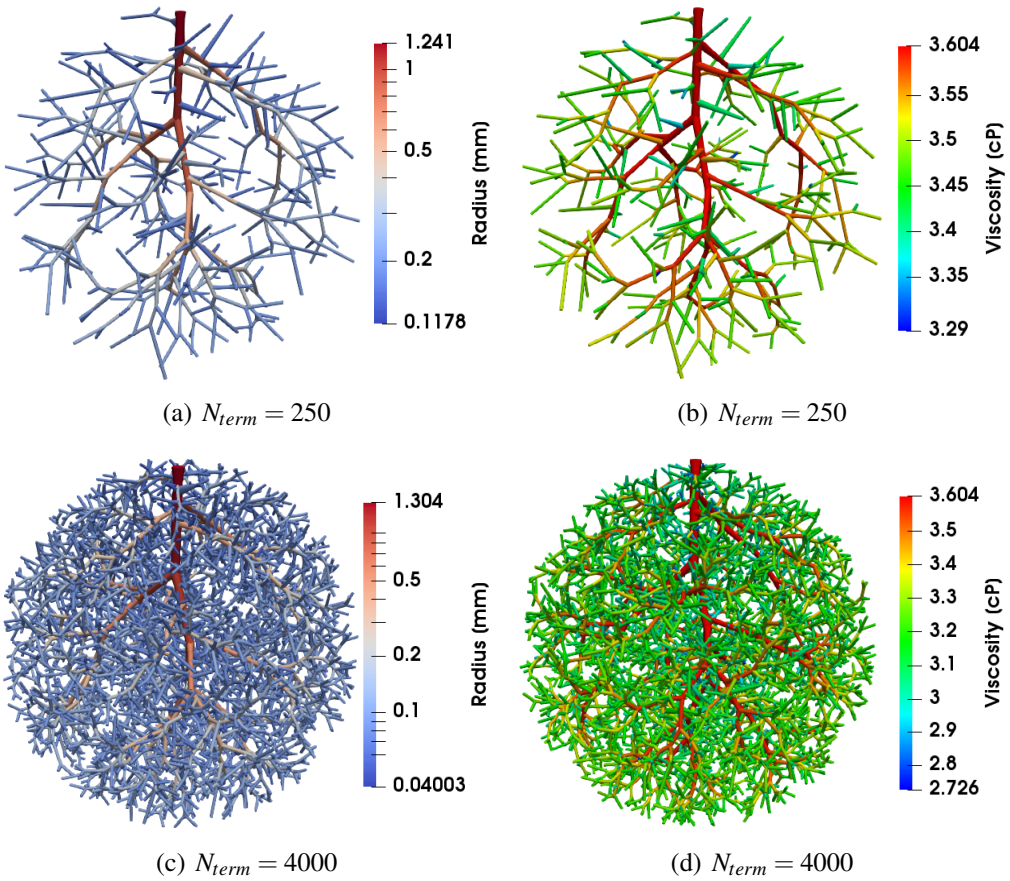

(a) $N_{term} = 250$ (b) $N_{term} = 250$

(c) $N_{term} = 4000$ (d) $N_{term} = 4000$

Figure 2: Visual representation of the models of an arterial tree with 250 and 4000 terminal segments.

4.2 Determining the root effective admittance of arterial tree models

In order to compare the root effective admittance of differents models of arterials trees, models were generated with 250, 500, 1000 and 2000 terminals segments using the Algorithm 1 and under the same conditions adopted in Section 4.1.

The following parameters were used to determine the root effective admittance Y_e^{iroot} of the models (DUAN; ZAMIR, 1995): the wall thickness of vessel $h_i = 0.05d_i$, Young's modulus $E = 1.0 \times 10^7\ dynes/cm^2$, density of fluid $\rho = 1055\ kg/m^3$ and frequency f varying of 0 Hz until 2000 Hz with increasing of 100 Hz.

Figure 4 shows the root effective admittance Y_e^{iroot} in function of the angular frequency for each model generated with linear (continuous line) and nonlinear (dashed line) viscosities. From this figure that depicts the admittance spectrum of the models, one can be observe that both the number of terminals and the viscosity influenced the root effective admittance. In particular, the increase in the number of terminals caused an increase in root effective admittance.

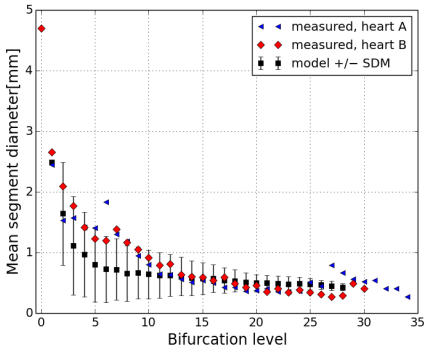

(a) constant viscosity 3.6 cP.

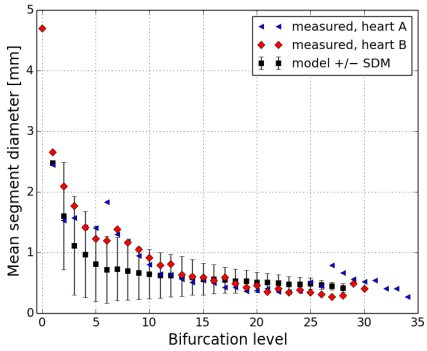

(b) variable viscosity given by Eq. (4).

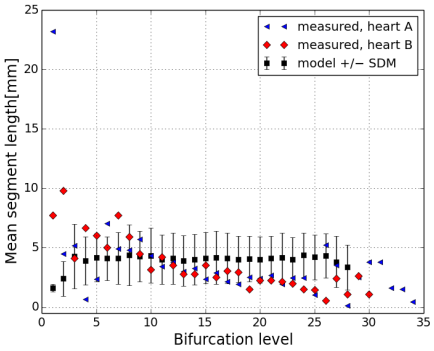

(c) constant viscosity 3.6 cP.

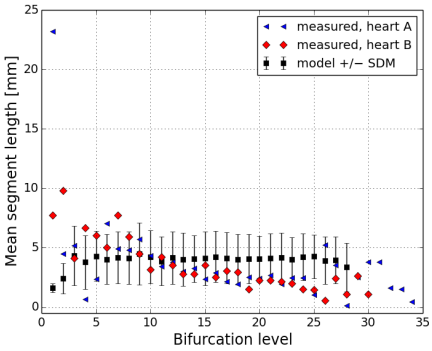

(d) variable viscosity given by Eq. (4).

Figure 3: Morphometric comparison between tree models and real left coronary arterial trees of two humans.

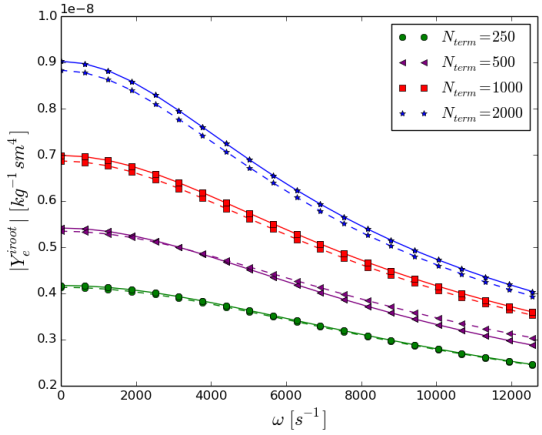

Figure 4: The root effective admittance of arterials trees with 250, 500, 1000 and 2000 terminals segments. The dashed line represented arterial tree models generated with variable viscosity given by Eq (4), and the continuous line represented models obtained with constant viscosity 3.6 cP.

5 Conclusion and future work

In this work, an algorithm based on CCO method is presented, which is capable of generating tree models taking into account the Fåhraeus-Lindqvist effect. These arterial tree models are in agreement with real vascular trees regarding morphometric parameter. In addition, the simulations presented here have the purpose to complement which had been done in Karch et al. (1999) using only constant viscosity. This work also showed results involving root effective admittance of the arterial tree models.

It should be emphasized that the described algorithm can be improved. In future work, we plan to incorporate elastic representation and collateralization of the vessels. Calculate the velocity (Eq. (12)) using a relationship between Young's modulus, wall thickness and radius of segment described by an exponential equation (OLUFSEN el at., 2000).

6 Acknowledgement

This work was partially supported by the Brazilian agency FAPEMIG which is gratefully acknowledged (Proc. Num. 00795-14).

7 References

BATCHELOR, G. K. **An introduction to fluid dynamics**. Cambridge: Cambridge University Press., 2000.

BRITO, P. F. **Construção de modelos de árvores arteriais considerando o efeito Fåhræus-Lindqvist**. 2016. 88 f. Dissertação - (Mestrado em Modelagem Computacional)- Universidade Federal de Juiz de Fora, Juiz de Fora, 2016.

BRITO, P. F. et al. Automatic construction of three-dimensional model of arterial tree incorporating the Fåhraeus-Lindqvist effect. In: ENCONTRO REGIONAL DE MATEMÁTICA APLICADA E COMPUTACIONAL, 4., 2017, Bauru. **Caderno de Trabalhos completos e resumos**. Bauru: UNESP, Faculdade de Ciências, 2017. p. 80-86.

DUAN, B.; ZAMIR, M. Pressure peaking in pulsatile flow through arterial tree structures. **Annals of Biomedical Engineering**, v. 23, n. 6, p. 794-803, 1995.

FÅHRAEUS, R.; LINDQVIST, T. The viscosity of the blood in narrow capillary tubes. **American Journal of Physiology**, v. 96, n. 3, p. 562-568, 1931.

KARCH, R. et al. A tree-dimensional model for arterial tree representation, generated by constrained constructive optimization. **Computers in Biology and Medicine**, v. 29, n. 1, p. 19-38, 1999.

MATES, R. E.; KLOCKE, F. J.; CANTY JR, J. M. Coronary capacitance. **Progress in Cardiovascular Diseases**, v. 31, n. 1, p. 1-15, 1988.

OLUFSEN, M. S. et al. Numerical simulation and experimental validation of blood flow in arteries with structured-tree outflow conditions. **Annals of Biomedical Engineering**, v. 28, n. 11, p. 1281-1299, 2000.

PRIES, A. R. et al. Blood Flow in Microvascular Networks, Experiments ans Simulation. **Circulation Research**, v. 67, n. 4, p. 826-834, 1990.

QUEIROZ, R. A. B. **Construção automática de modelos de árvores circulatórias e suas aplicações na hemodinâmica computacional**. 2013. 196 f. Tese (Doutorado em Ciências em Modelagem Computacional)- Laboratório Nacional de Computação Científica, Petrópolis, 2013.

SCHREINER W.; BUXBAUM, P. Computer-optimization of vascular trees. **IEEE Transactions on Biomedical Engineering**, v. 40, n. 5, p. 482-491, 1993.

SCHWEN, L. O. et al. Algorithmically generated rodent hepatic vascular trees in arbitrary detail. **Journal of Theoretical Biology**, v. 365, p. 289-300, 2015.

VAN BEEK, J. H. G. M.; ROGER, S. A.; BASSINGTHWAIGHTE, J. B. Regional myocardial flow heterogeneity explained with fractal networks. **American Journal of Physiology**, v. 257, n. 5, p. H1670-H1680, 1989.

WATANABE, S. M.; BLANCO, P. J.; FEIJÓO, R. A. Mathematical model of blood flow in anatomically detailed arterial network of the arm. **ESAIM: Mathematical Modelling and Numerical Analysis**, v. 47, n. 4, p. 961-985, 2013.

YANG, J.; WANG, Y. Design of vascular networks: a mathematical model approach. **International Journal for Numerical Methods in Biomedical Engineering**, v. 29, n. 4, p. 515-529, 2013.

ZAMIR, M. Distributing and delivering vessels of the human heart. **The Journal of General Physiology**, v. 91, n. 5, p. 725-735, 1988.

ZAMIR, M. **The physics of pulsatile flow**. New York: Springer, 2000.

ZAMIR, M.; CHEE, H. Segment analysis of human coronary arteries. **Blood Vessels**, v. 24, p. 76-84, 1987.

Artigo recebido em jun. 2017 e aceito em nov. 2017.